Development of an Inverted Optical Tweezers with Full Motional Control

Hamsa Sridhar

Kings Park High School

International Science and Engineering Fair

Physics Individual Project PH019

May 13, 2007

1 Introduction

Optical tweezers, or laser traps, were first introduced by Ashkin in the 1980s (Ashkin et al., 1986). Using focused light rays, they allow the non-invasive trapping and manipulation of micro-particles in all three dimensions.

Optical tweezers are used frequently in biological applications such as isolating cells and their organelles (Leitz et al., 2003) or micro-manipulating cells to redirect their growth (Erlicher et al., 2002). In this setup, regular yeast cells, immersed in tap water, were manipulated.

2 Optical Trapping Theory

Electromagnetic radiation carries energy and momentum. An interaction between this radiation and matter can result in the transfer of linear momentum to the particle (Hu et al., 2007). This principle is the underlying basis of laser-activated traps that confine atoms or particles in the Mie Regime, where particle diameter >> wavelength of laser beam (Wright et al., 1994).

Laser traps, more commonly referred to as optical tweezers, use a single-beam laser to transfer momentum and manipulate micron-sized particles in a fluid medium. For optimal trapping, the index of refraction of the particle must be greater than that of the surrounding medium. When a light ray passes through the particle, it refracts and the photons' velocity and momentum decrease. The change in momentum exerts a series of forces on the particle that are governed by the direction in which the light refracts – forces act in opposite reactionary pairs so when the particle causes the light to refract down, the light exerts an upward force on the particle.

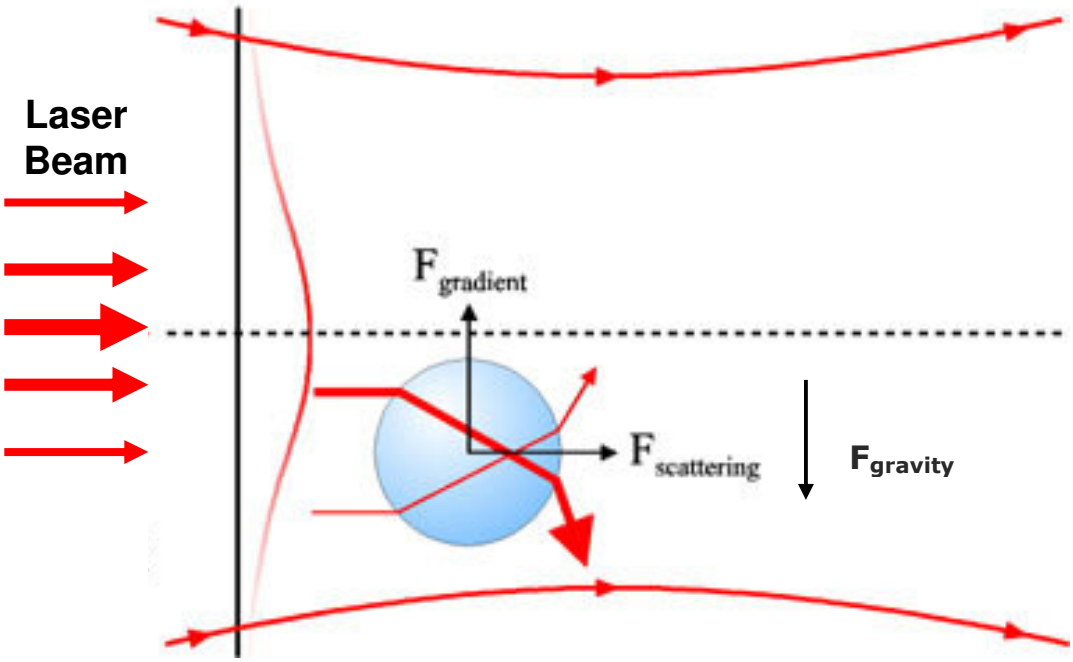

Fig. 1: The thicker arrows represent a higher intensity than the thinner ones. When the light rays pass through the particle, they refract and a gradient force, caused by the higher intensity rays, always pushes the particle towards the focus while the scattering force pushes the particle in the direction of propagation. Gravity always exerts a downward force on the particle (Optical Tweezers: An Introduction, 2006).

The key forces acting on the particle can be classified as the gradient force, the scattering force, and the force of gravity (Fig.1). The gradient force is caused by the light's Gaussian intensity profile where the center has the highest light intensity (Fig.2).

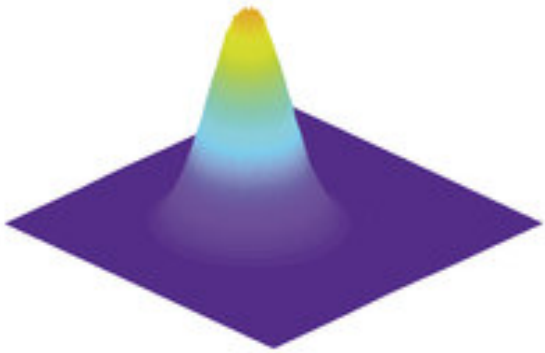

Fig.2: The laser beam's Gaussian intensity profile makes the beam very intense in the center. Force exerted when these central rays refract, causes the dominant gradient force which pulls the particle towards the focus of the beam.

The gradient force acts towards the focus of the light beam (Fig.1) and is called the restoring force as it pulls the particle towards the point of highest intensity, thereby trapping it. The stronger the net gradient force, the stronger the trap (Wright et al., 2007). The scattering force is caused by the radiation pressure exerted in the direction that the beam travels and so this force always acts in the direction of the laser beam's propagation. The third force is the force of gravity which perpetually pushes the particle downwards.

As the intensity of the focus increases, the magnitude of the forces, exerted on the particle by the beam, increases. The intensity of the focus can be maximized through careful alignment procedures that ensure that the highest beam intensity enters the aperture of the objective that is used to focus the beam onto a particle.

2.1 Regular vs. Inverted Tweezers

In a regular optical tweezers, the laser is positioned above the sample and the light moves downward to trap the particle so the scattering force acts downwards, along with the force of gravity. Thus, the gradient force, which pulls the particle to a single point, thereby trapping it,

must counteract both the scattering force and gravity (Fig.3a). To create a gradient force strong enough to trap cells while counteracting these forces requires a high power laser.

Since the laser used in this project was an inexpensive one with 23mW power, an inverted optical tweezers setup was created to maximize the net gradient force produced in order to trap particles. In an inverted optical tweezers, the laser is positioned underneath the sample and the laser beam travels upward. As a result, the scattering force also acts upwards while gravity pulls the particle downwards. So, the scattering force and gravity act against each other and the gradient force compensates less for the other two undesirable forces (Fig. 3b). Consequently, the net gradient force is greater and the trap is stronger, allowing a laser of lower power to trap and manipulate particles.

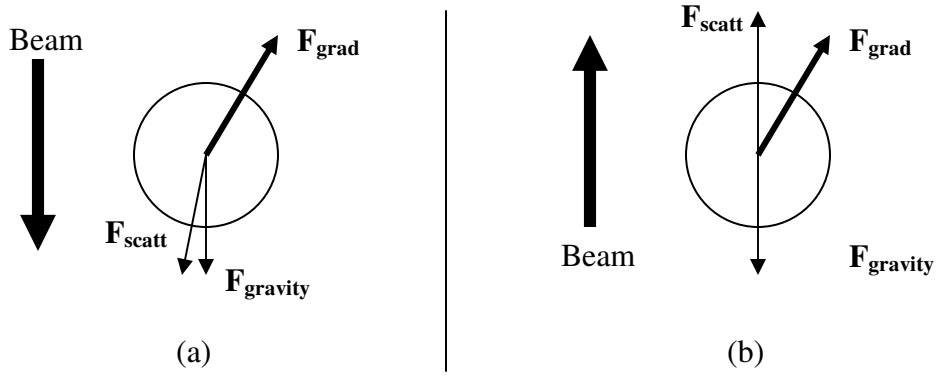

Fig. 3: (a) Regular optical tweezers: The laser beam travels down so both the scattering force and gravity act down while the gradient force has to compensate for both to push the particle towards the focus and trap it. (b) Inverted optical tweezers: The beam travels up so the scattering force acts against gravity and the gradient force compensates less for the two.

The net force acting on a particle by the tweezers, or the trapping efficiency, can be gauged by measuring the maximum velocity at which a particle can be dragged by the tweezers

in the fluid medium, commonly known as drag velocity. This can then be used to calculate the drag force exerted, using Stokes' equation.

2.2 Yeast Cells

Yeast cells were the chosen sample particles for trapping and manipulating. The experiment was conducted in the Mie Regime as the particle diameter, approximately 10μm for a yeast cell, is much greater than the wavelength of the He-Ne red laser beam used.

Yeast cells have a greater index of refraction than water, the fluid medium in which the yeast cells were placed. Thus, incident light would refract and the gradient force necessary for trapping would be produced. Moreover, yeast cells are transparent so more light would transmit and refract, rather than reflect, increasing the gradient force exerted.

2.3 Purpose

The purpose of this project was to develop a working inverted optical tweezers setup, to optimize the gradient force, and to measure the drag force exerted by the setup when trapping and manipulating yeast cells three-dimensionally.

3 Design and Construction of Optical Tweezers

In this section, the methods for constructing the optical tweezers setup and the various measurements made to optimize the focused laser beam and increase the gradient force is discussed.

3.1 Setup

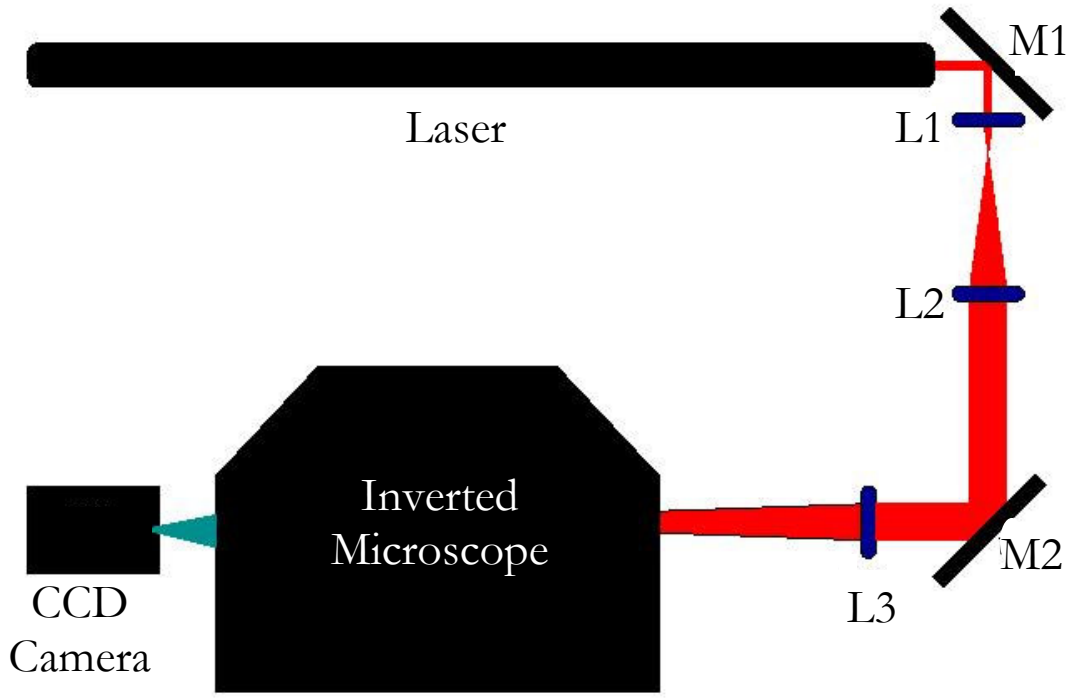

Fig.4: The aerial view of the setup is shown. M_1, and M_2 are regular gold plane mirrors. L_1, L_2, and L_3 are plano-convex spherical lenses. The red light is the laser beam and the green light issuing from the inverted microscope into the CCD camera is the white illumination light which has been passed through a green filter.

The laser beam emitted from the laser was collimated and was reflected off of the first gold plane mirror. It was then sent into a telescope, consisting of two lenses, where it was resized and re-collimated. The beam was then reflected off of the second mirror and was sent into the third lens (Fig.4).

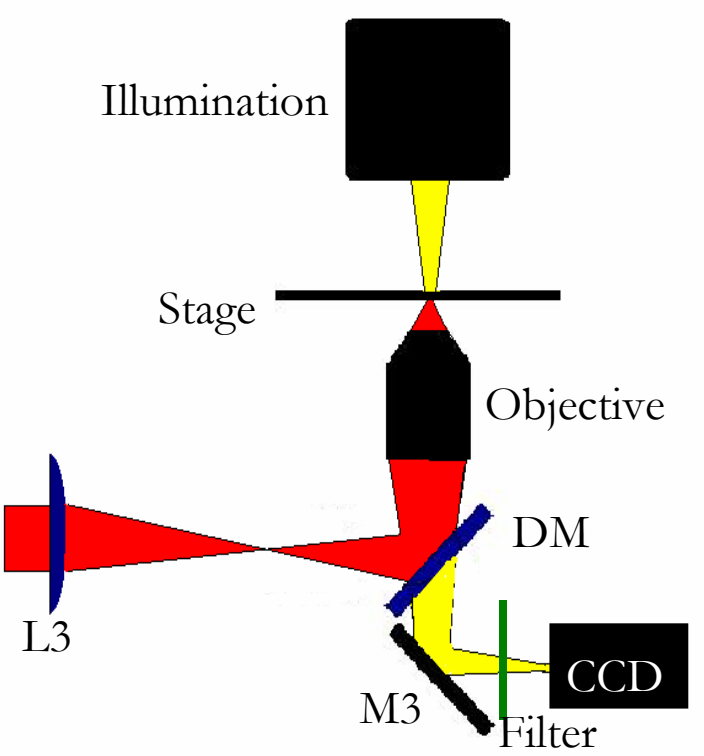

Fig.5: The side view of the microscope is shown with the red laser beam entering from the third lens and the white illumination light (represented as yellow) emitting from the illumination above the stage and entering the CCD camera through a green filter. D_1 and D_2 are dichroic mirrors.

The third lens converged the beam and brought it to a focus 160mm before it reflected off of a dichroic mirror (a specially coated mirror that transmits and reflects certain wavelengths of light depending on the angle of incidence) and entered the objective. The objective focused the beam onto the stage where the sample of yeast cells was placed.

The illumination light emitted from a Kohler illumination LED was focused onto the stage. Then, it passed through the objective, transmitted through the dichroic mirror, reflected off of the third mirror, and came to a focus on the CCD element 160mm away. A green filter was placed before the CCD camera to eliminate stray laser reflections entering the camera.

3.2 Optical Elements

A red He-Ne laser beam with wavelength 632.8 nm, 23mW power, and a partially Gaussian intensity profile, was used. Three gold plane mirrors were used to reflect the beam with attached micrometer knobs to adjust the angle of reflection in all three dimensions. Plano-convex spherical lenses were used, having focal lengths of 25.4mm, 150mm, and 170mm respectively. A dichroic mirror, which reflected 80% of He-Ne red light and transmitted regular white light incident at a 45-degree angle, was used to separate the two wavelengths of light as they both passed through the objective. The objective was 40x and had a numerical aperture of 0.85. A Nikon inverted microscope was used and a Kohler illumination LED was attached above the microscope to provide light for imaging. A CCD camera without a focusing lens was used and so the beam was brought to a focus directly on the CCD element.

3.3 Alignment

The laser beam's path was carefully aligned in all three dimensions to ensure that the highest beam intensity entered the objective. Higher intensity in turn would produce a stronger gradient force on the particle, strengthening and optimizing the trap.

The laser and all other optical elements were screwed into an optical table and kept at low heights to avoid vibrational aberrations and increase stability. A level was used to ensure that all optical elements, especially the laser, were perfectly horizontal.

Horizontal laser alignment was verified by measuring the vertical height of the beam just after the mirror and after a short distance away. These heights should be the same if the laser's path did not deviate from the horizontal xy-plane. Micrometer knobs were used to three-dimensionally adjust the plane of the mirror, hence the alignment of the beam, until these heights were the same.

Similarly, the lenses were placed on a translational stage with micrometers. The laser beam's diameter after exiting the first two lenses was measured both initially and after traveling a distance away. Both diameters had to be equal if the beam was collimated and this was ensured by adjusting the distance between the two lenses. Also, to verify that the lenses were exactly orthogonal to the beam, the lens reflections were checked and adjusted until they traveled straight back into the laser.

3.4 Increasing the Intensity of Steep Light Rays

Light rays entering the objective, and later the particle, at steep angles undergo more refraction and thus exert more gradient force on the particle. To increase the gradient force, the light rays entering at steep angles should have a high intensity. However, at the same time, the total intensity of the beam entering the objective should also be maximized so that the focus has increased intensity and the trapping forces are maximized. To determine the appropriate central section of the beam that should enter the objective, the beam profile was measured.

3.4.1 Measuring the Laser Beam Profile

The laser beam's profile was measured using the pin-hole method. A small hole was translated across the width of the laser beam, one thousandth of an inch at a time, and a photodetector was used to measure the intensity of the laser at each point (Fig.6). The data was then graphed to form the beam profile (Fig.7).

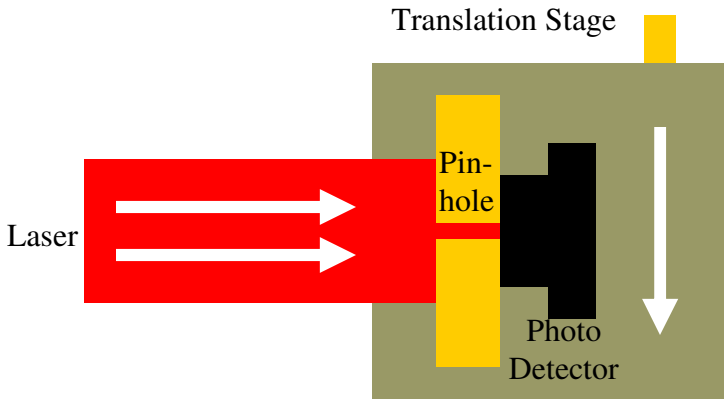

Fig.6: The beam profile measurement was made using the above apparatus. The intensity of the laser beam across its cross-section was measured using a photo detector, one thousandth of an inch at a time.

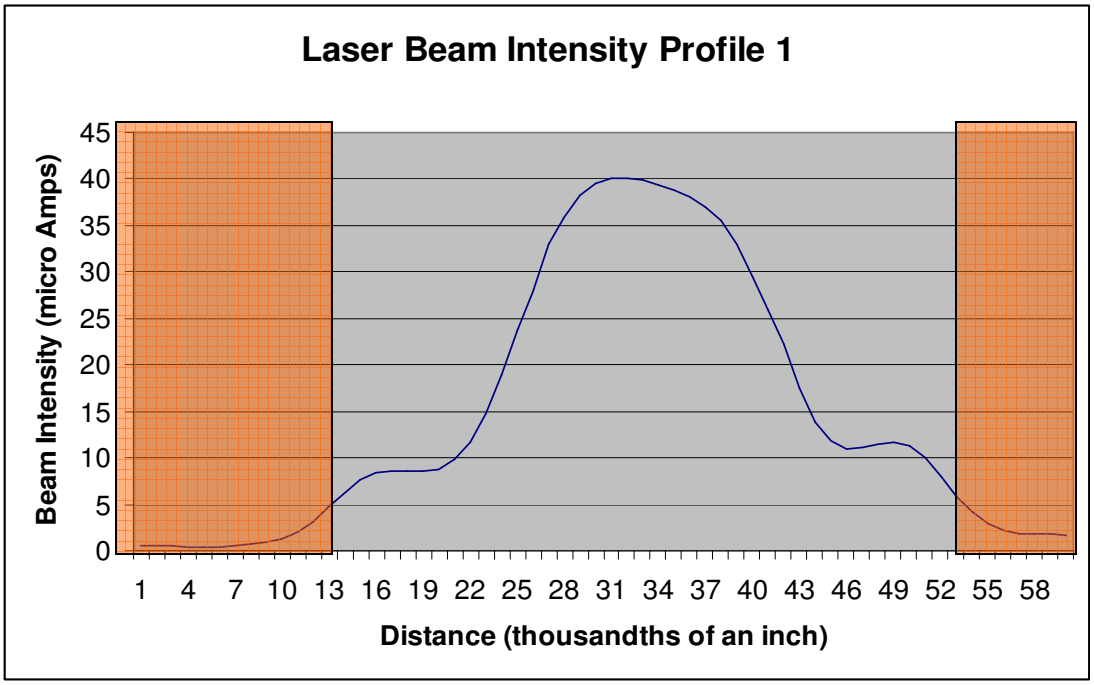

Fig.7: The curve represents the beam's intensity profile. The part of the laser beam that isn't shaded would be the ideal part to enter the objective as the small high intensity peaks enter the objective from the steepest angles, increasing refraction and the gradient force. The central component of the beam ranges from 13 to 53: a width of approximately 40 thousandths of an inch.

In contrast with a regular Gaussian curve (Fig.2), small high intensity peaks were found at the ends of the beam profile. Since these peaks would maximize the intensity of the light rays entering the objective at the steepest angles, they were included in the desired central section of the beam to enter the objective, marked by the unshaded region (Fig.7).

These measurements were then repeated after the laser was rotated 90 degrees, using the same pinhole method (Fig.8).

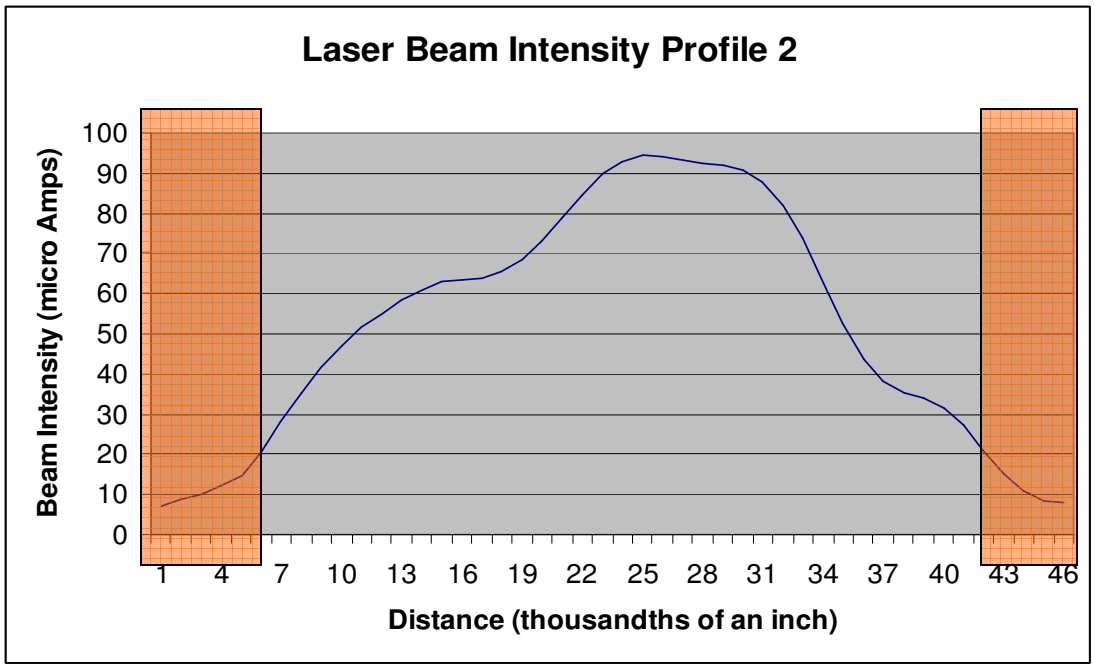

Fig.8: The curve represents the beam's intensity profile after rotating the laser 90^{o}. High intensity peaks are still apparent at the sides and these are incorporated in the desired central component again, ranging from 6 to 43: a width of approximately 37 thousandths of an inch.

Due to the high intensity peaks found on the sides of the beam profile, the ideal central component of the beam to enter the objective was determined to have a width of approximately 40 thousandths of an inch in both measurements. This central width had to be enlarged to fill the aperture of the objective, which was 6mm wide.

3.4.2 Telescope

The central region of the beam, determined earlier to be 40 thousandths of an inch, approximately 1.02mm, had to be expanded approximately 6 times to fill the 6mm wide aperture of the objective. This was done by creating a telescope using two plano-convex (to reduce spherical aberrations) lenses of focal length ratio 1:6. The laser beam was passed through lenses of focal lengths 25.4mm and 150mm respectively; the lenses were separated by a distance of the sum of their focal lengths – 175.4mm so that the collimated beam that entered the telescope would also leave collimated (Fig.9).

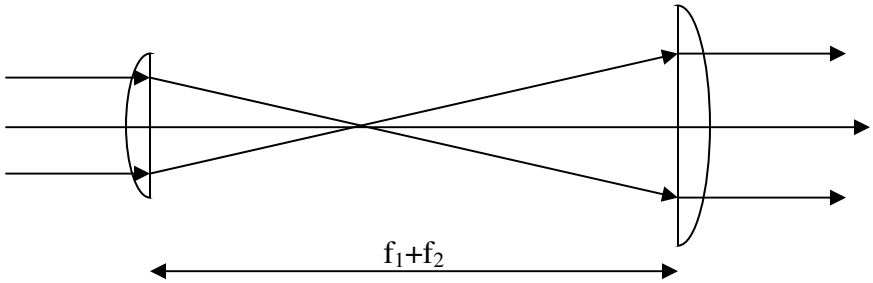

Fig.9: The laser beam passes through the 25.4mm focal length lens and then the 150mm focal length lens. The two lenses are separated by a distance of f_1+f_2 so that the beam exits the telescope collimated again and the beam is expanded to 6 times its original width.

3.5 Sample and Rose Chamber

The yeast cells, immersed in water, were placed on a standard glass slide. To achieve three-dimensional trapping and manipulation, a rose chamber was created to add depth to the slide. A doughnut-shaped hole was cut in the center of a square of 100µm-thick parafilm. The parafilm square was then sealed onto a glass slide using a heat gun. The yeast cells were then placed within the chamber created by the hole in the parafilm and a Size 0 cover slip (100µm-thick) was

placed on top. The glass slide was then placed upside down on the stage of the inverted microscope (Fig.10).

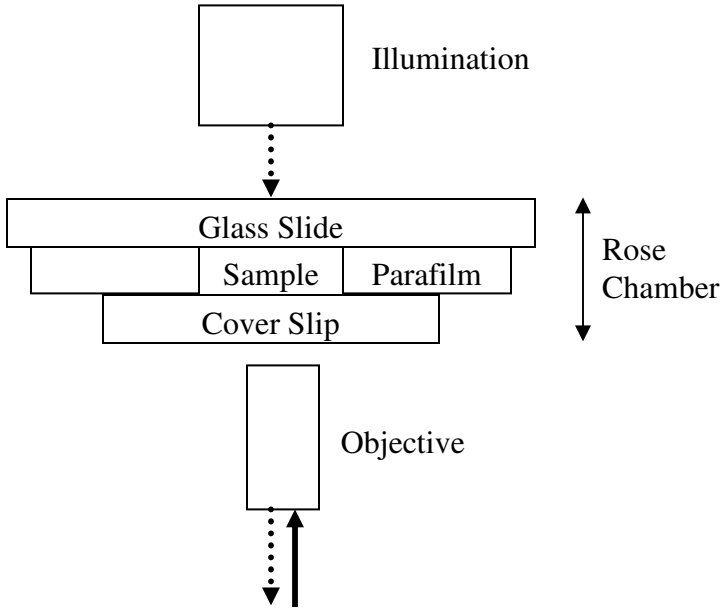

Fig.10: The illumination light is represented by the dotted arrows. It passes through the rose chamber and exits through the objective while the laser beam, represented by the solid arrow, passes through the objective, and comes to a focus inside the rose chamber.

3.6 Imaging

The yeast cells and the focus of the laser beam were imaged using a CCD camera. The white illumination light was provided by the Kohler illumination attached above the inverted microscope. The light traveled through the rose chamber and entered the CCD camera. However, the camera required an expensive long focal length lens to focus the imaging light onto the CCD element. So the original short focal length lens on the camera was removed and instead of using a focusing lens, the illumination light was brought to a focus directly onto the CCD element. As the objective was 40x, the illumination light converged to a focus 160mm after exiting the objective, which was where the camera was placed.

The laser beam and the illumination light had to follow the same path entering and exiting the objective respectively so that when the CCD camera was imaging a certain depth in the rose chamber, the focus of the laser beam would also be on the same horizontal plane. Thus, a third lens was used in the setup with a focal length of 170mm (Fig.5). It brought the laser beam to a focus 160mm before entering the objective so that it followed the same path as the illumination.

The video input from the CCD camera was projected onto a standard black-and-white monitor for observation of the laser trap. The total magnification was measured to be 1750x.

4 Trapping and Calculations

In this section, the methods of trapping and manipulating the yeast cells three-dimensionally are described. Moreover, calculations measuring the power efficiency of the setup and the drag force exerted by the setup on the cells in all three dimensions are examined.

4.1 Optical Trapping and Manipulation

The laser beam was focused and directed into the sample. By adjusting the microscope stage until the yeast cells were in focus, the intended plane of view was obtained. From that position, the laser beam was manipulated onto a specific cell to trap it.

After trapping a particle, the focus of the laser beam was manipulated to change the direction of the gradient force, which in turn moved the particle. By slightly changing the angle of the laser beam's propagation with one of the micrometer knobs on the second mirror, the focus and the particle was moved on the xy-plane. For three-dimensional trapping, or movement along the z-axis, the distance between the laser's focus and the stage was altered slightly by turning the micrometer on the fine adjustment knob of the microscope.

The trapping distance of the trap was approximately 5μm and stability of a trapped particle lasted for more than an hour.

4.2 Power Efficiency

A power meter was used to measure the power of the laser beam after every optical element (see Fig.11).

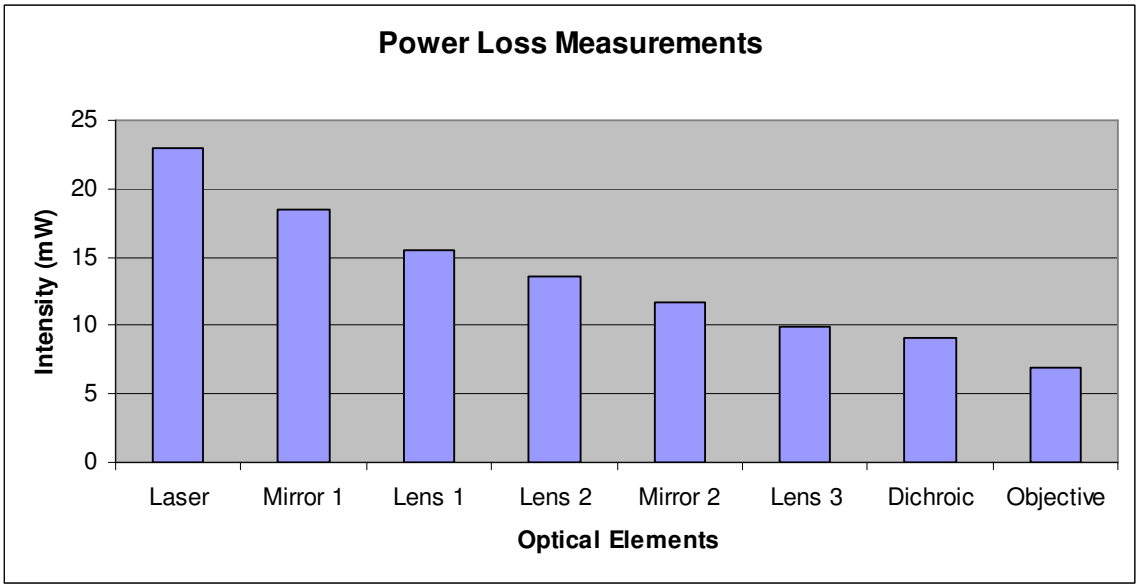

Fig.11: The graph shows the power of the beam after each optical element. The initial power of 23 mW was eventually reduced to 7 mW as the beam exited the objective.

No particular optical element greatly reduced the power of the setup. Starting with 23 mW and ending with 7 mW, the setup had an overall power efficiency of approximately 30%. The 7 mW power that exited the objective exceeded the minimum 5 mW power needed to trap 10μm-diameter particles, such as yeast cells (Wright, 1990).

4.3 Drag Force

The trapping efficiency of an optical tweezers setup can be gauged by the highest velocity at which a particle can be dragged in the fluid medium by the laser's focus – the drag velocity. This

can be used to calculate the net drag force that the beam exerts on the particle to manipulate it in a given dimension (O'Neal and Padgett, 2001).

Stokes' equation for drag force at low velocities is:

$$\mathbf{F_d = -6\Pi\eta rv}$$

η is the fluid viscosity which is 10^{-3} for water, the medium used.

r is the radius of the particle, which is approximately 5μm for yeast cells.

v is the drag velocity.

4.3.1 XY-Plane

The drag velocity of the particles was calculated by determining the maximum distance a cell could be dragged in the horizontal plane using the tweezers in a given interval of time. The distance was measured directly on the monitor and was divided by 1750 to account for the magnification. The average drag velocity was 10 μm/sec. Thus, using Stokes' equation, the drag force exerted by the trap was 0.9 pN.

4.3.2 Swimming Pool Effect

A similar method for calculating the drag velocity at the z-axis was used. For manipulation in the third dimension, the stage was lowered by using the micrometer on the fine adjustment knob of the microscope, thereby moving the focus of the laser beam up inside the chamber. However, due to aberrations caused by refraction, the distance the stage was lowered did not equal the distance the focus moved up inside the chamber. This difference was especially significant at high angles of incidence (see Fig.12).

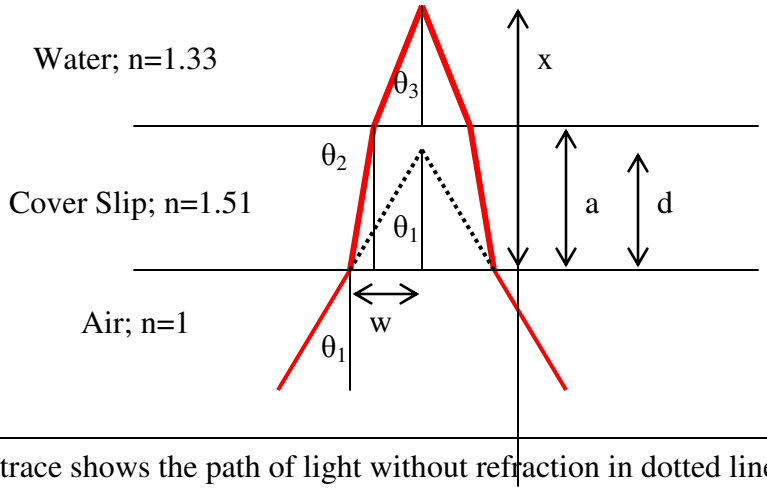

Fig.12: The ray trace shows the path of light without refraction in dotted lines while the actual path is shown in red. The light refracts between two interfaces: air-cover and cover-water.

Thus, an equation was created to model the distance the focus moved up, Δx, for any particular value, d, that the stage was lowered, depending on the angle of incidence of the light rays. a is the height of the cover slip (100μm) and θ is the incident angle of the light ray.

$$n_1\sin\theta_1 = n_2\sin\theta_2 \textit{ and } n_2\sin\theta_2 = n_3\sin\theta_3 = n_1\sin\theta_1 \textit{ by Snell's Law}$$

$$\theta_2 = \sin^{-1}((n_1/n_2)\sin\theta_1) \textit{ and } \theta_3 = \sin^{-1}((n_1/n_3)\sin\theta_1)$$

$$w = d*\tan\theta_1 = a*\tan\theta_2 + (x-a)*\tan\theta_3$$

$$\mathbf{x = (d*\tan\theta_1 - a*\tan(\sin^{-1}((n_1/n_2)\sin\theta_1))) / \tan(\sin^{-1}((n_1/n_3)\sin\theta_1)) + a}$$

Since the numerical aperture (NA) of the objective is 0.85 = nsinθ, the maximum angle at which a beam could enter the objective is 58°. The distance the focus moves up (x) for any angle of incidence (θ_1) between 0° and 58° was calculated and graphed for the stage moving distances (d) of 80, 90, and 100μm (Fig.13).

Fig.13: The graph shows the distance the focus moved up (x) in microns for differing angles of incidence. The three lines show results for d = 80, 90, and 100μ.

Thus, when the stage moves up 10μm, the focus moves up 13μm (Δx) for the central rays, with low values of θ_1, and 19μm (Δx) at the steepest angles, with high values of θ_1. On average, it can be assumed the focus moves up 16μm for every 10μm the stage is moved.

4.3.3 Drag Force in the Z-Axis

Using the above calculation, the drag velocity was measured for the z-axis in the same method as that for the xy-plane and was approximately 1.14μm/sec. Using the Stokes' equation, the net drag force was 0.1pN.

However, unlike movement in the xy-plane, the gravitational force acts against upward movement in the z-axis. The velocity of a particle falling to the bottom of the chamber was

measured to be 3.2μm/sec. Using Stokes equation again, gravity exerts a 0.3pN force downwards on the particle.

Thus, since the net force is 0.1pN up with gravity exerting a force of 0.3pN down, the tweezers actually exert a drag force of 0.4pN up.

5 Summary and Conclusions

A working optical tweezers setup was created and optimized by maximizing the gradient force. Yeast cells were successfully trapped and manipulated three-dimensionally. The trap's radius of control was approximately 5μm and the stability of the trap lasted greater than an hour. Thirty percent power efficiency was achieved by careful alignment procedures. The tweezers exerted a 0.9pN force when manipulating particles on the xy-plane and a 0.4pN force when manipulating particles up the z-axis. Both forces were within the required range for optical manipulation techniques in the biological field (Wang, 1999).

6 References

Ashkin A., Dziedzic J.M., Bjorkholm J.E., Chu S. 1986. Observation of a single-beam gradient force optical trap for dielectric particles. *Optical Letters*. 11: 288–290.

Leitz, G., Lundberg, C., Fallman, E., Axner, O., Sellstedt, A. 2003. Laserbased micromanipulation for separation and identification of individual Frankia vesicles. *FEMS Microbiology Letters*. 224: 97–100.

Erlicher, A., Betz, T., Stuhrmann, B., Koch, D., Milner, V., Raizen, M.G., Kas, J. 2002. Guiding neuronal growth with light. *Proc. National Acad. Science USA*. 99: 16024-16028.

Zhaohui Hu, Jia Wang and Jinwen Liang. 2007. Experimental measurement and analysis of the optical trapping force acting on a yeast cell with a lensed optical fiber probe. *Optics & Laser Technology.* 39: 475-480

Wright, W.H., Sonek, G.J., and Berns, M.W. 1994. Parametric study of the forces on microspheres held by optical tweezers. *Applied Optics.* 33: 1735.

Optical Tweezers: An Introduction. <http://www.stanford.edu/group/blocklab/Optical%20Tweezers%20Introduction.htm> Accessed 25 Feb 2007.

Graham D. Wright, Jochen Arlt, Wilson C.K. Poon and Nick D. Read. 2007. Optical tweezer micromanipulation of filamentous fungi. *Fungal Genetics and Biology*. 44: 1-13.

Wright, W.H., Sonek, G.J., Tadir, Y., and Berns, M.W. 1990. Laser Trapping in Cell Biology. *IEEE Journal of Quantum Electronics.* 26: 12: 2148-2157.

O'Neal, Anna T. and Padgett, Miles J. 2001. Axial and lateral trapping efficiency of Laguerre-Gaussian modes in inverted optical tweezers. *Optics Communications.* 193: 45-50.

Wang, Michelle D. 1999. Manipulation of single molecules in biology. *Current Opinion in Biotechnology.* 10: 81-86.